Available online at www.sciencedirect.com

ScienceDirect

Procedia IUTAM 16 (2015) 33 – 40

Procedia IUTAM

www.elsevier.com/locate/procedia

IUTAM Symposium on Dynamics of Capsules, Vesicles and Cells in Flow

Thin-film flow beneath a vesicle during adhesion processes

Maurice J. Blount[a,b,*], Michael J. Miksis[b], Stephen H. Davis[b]

[a]*School of Mathematics, Cardiff University, Senghennydd Road, Cardiff CF24 4AG, UK*
[b]*Engineering Sciences and Applied Mathematics, Northwestern University, 2145 Sheridan Road, Evanston IL 60208, USA*

Abstract

Lubrication theory is used to model the dynamics of a vesicle as it adheres to a rigid horizontal substrate. Travelling-wave solutions are obtained and used to estimate the spreading of the vesicle along the substrate. The results are compared with boundary-integral simulations, and good agreement is demonstrated in cases where the vesicle's shape is already close to its equilibrium shape. In the more general case, there is a transient motion that is not described by scalings obtained using lubrication theory.

Peer-review under the responsibility of the organizing committee of DYNACAPS 2014 (Dynamics of Capsules, Vesicles and Cells in Flow).

Keywords: adhesion, lubrication flow, boundary-integral simulations

1. Introduction

Particulate suspensions are commonplace in industrial and biological situations, and microscale interactions between suspended particles can affect macroscopic properties of the flow. Recent experiments have measured the interaction forces between two vesicles as they adhere and as they are subsequently pulled apart[1], and other experiments have measured the temporal variation in the contact area of an adhered vesicle as it is pulled off of a substrate[2]. In both situations, it is thought that hydrodynamic effects play an important role both during adhesion and during separation. Recent theoretical work has analysed the equilibrium configurations of a pair of vesicles in the regime where the adhesive interaction is strong enough to dilate the membrane[3], in which case the membrane's bending stiffness is not dynamically important. Here, we analyse the process by which a vesicle adheres to a rigid substrate, in the regime where the adhesive interaction is not strong enough to dilate the vesicle's membrane appreciably. In this regime, the membrane may be modelled as inextensible, with its tension varying spatially in response to tractions exerted on it by the surrounding fluid, and the dynamics are governed by a balance between adhesion and the membrane's bending stiffness.

The equilibrium shapes of a vesicle that is adhered to a substrate have been analysed by modelling the adhesive interaction as a contact potential[4], but a drawback of using such a model to describe dynamic processes is that any motion of the contact line would give rise to a non-integrable singularity in the viscous stresses there, known as

* Corresponding author. Tel.: +44-292-087-0617 ; fax: +44-292-087-4199.
E-mail address: BlountMJ@cardiff.ac.uk

Peer-review under the responsibility of the organizing committee of DYNACAPS 2014 (Dynamics of Capsules, Vesicles and Cells in Flow).
doi:10.1016/j.piutam.2015.03.005

the 'contact-line singularity'[5]. We therefore analyse the case where the adhesive interaction is finite-ranged, so that in equilibrium there is a thin wetting layer of fluid beneath the vesicle. The effect of such a wetting layer on the equilibrium shapes of such vesicles has been analysed[6], and here we analyse the dynamic behaviour as the vesicle spreads along the substrate. Our approach is similar to an earlier analysis of cell adhesion[7], but here we include the effects of the membrane's bending stiffness. We begin in Sec. 2 by formulating the problem, and briefly summarise a recent analysis of vesicles in equilibrium in the presence of finite-ranged adhesive forces. This work motivates the use in Sec. 3 of lubrication theory to describe the spreading of a vesicle as it adheres to a substrate, and the predictions of this model are compared against estimates obtained using a boundary-integral technique. The results and possible avenues for further work are discussed in Sec.4.

2. Formulation of problem

Throughout the following we denote dimensional quantities using asterisks and dimensionless quantities using undecorated variables. We focus on a two-dimensional vesicle, and model it as a closed, inextensible and impermeable bilipid membrane of perimeter P^* and bending stiffness κ^*. We nondimensionalise lengths with P^*, energies with κ^* and pressures with the corresponding scale κ^*/P^{*3}. We nondimensionalise times using the timescale given by $T^* = \mu^* P^{*3}/\kappa^*$, where μ^* is the dynamic viscosity of the fluid outside the vesicle, and velocities with the corresponding scale $\kappa^*/\mu^* P^{*2}$. We assume that there is an adhesive interaction between the membrane and the substrate that is long-range attractive, short-range repulsive, and that depends only on the distance y of the membrane above the substrate. We represent this interaction phenomenologically using the potential (expressed in dimensionless variables)

$$W(y) = W_0\left[\left(\frac{\delta_A}{y}\right)^4 - 2\left(\frac{\delta_A}{y}\right)^2\right], \tag{1}$$

where W_0 represents the strength of the adhesive interaction and is given by $W_0^* P^{*2}/\kappa^*$, where W_0^* is the energy of adhesion per unit membrane area, and δ_A represents the preferred distance between the membrane and the substrate (in the absence of any force other than the adhesive interaction) and is given by δ_A^*/P^*. The potential (1) has been constructed so that it is minimised at $y = \delta_A$ and so that its value there is given by $W = -W_0$. Although the quantitative results of our analysis depend on the specific form (1) used for $W(y)$, we anticipate that the qualitative results will hold for any potential that is short-range repulsive and long-range attractive.

The membrane exerts a traction on the surrounding fluid, which causes there to be a difference between the viscous stresses on either side of the membrane that is given by[8]

$$\boldsymbol{\sigma}\cdot\boldsymbol{n}|_{\text{out}} - \boldsymbol{\sigma}\cdot\boldsymbol{n}|_{\text{in}} = -\left(\frac{\mathrm{d}^2 H}{\mathrm{d}s^2} + \frac{1}{2}H^3 - WH - \boldsymbol{n}\cdot\boldsymbol{\nabla}W - \gamma H\right)\boldsymbol{n} - \frac{\mathrm{d}\gamma}{\mathrm{d}s}\boldsymbol{t}, \tag{2}$$

where s is the arclength measured anticlockwise along the membrane, $\boldsymbol{n}$ is the outward normal to the membrane and $\boldsymbol{t}$ is the tangent to the membrane in the direction of increasing arclength (see Fig. 1). The curvature H of the membrane

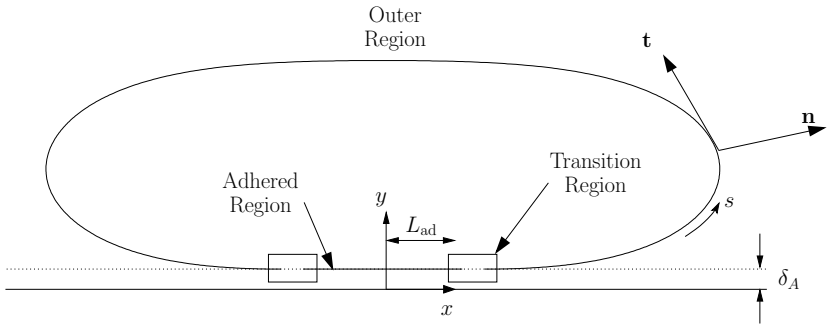

Fig. 1. Schematic diagram showing the geometry of the problem, and the separation of a vesicle's membrane into outer, adhered and transition regions (see text).

is defined by $\mathrm{d}\boldsymbol{t}/\mathrm{d}s = -H\boldsymbol{n}$. We note that here, in contrast to a fluid–fluid interface, γ is not an intrinsic property of the interface but instead varies spatially as necessary to enforce the constraint that the membrane's length be locally conserved. It must therefore be solved for as part of the problem. The form of the adhesive contributions to (2) are derived using the variational derivative of the adhesive energy, $\int W\,\mathrm{d}s$, with respect to the position of the surface (so that tangential displacements would produce no energy change). From (2), it follows that defining the adhesive stresses in this way means that γ must be spatially constant in order for the vesicle to be in equilibrium.

2.1. Equilibrium shapes

The equilibrium shape of a vesicle that is adhered to a substrate has previously been analysed[6] in the regime where $0 < \delta_A \ll 1$, and we briefly summarise the results here before analysing the dynamics. In the limiting case that $\delta_A = 0$, the adhesive potential represents a contact potential, and the membrane has two distinct regions; a flat 'adhered region' that is in contact with the substrate, and an 'outer' region where the adhesive potential is zero. It can be shown[4] that minimisation of the membrane's free energy with respect to the position of the contact point implies that in equilibrium, the membrane meets the substrate with a contact angle of π and curvature given by $H_c = (2W_0)^{1/2}$. If, instead, $0 < \delta_A \ll 1$ then the adhered region instead lies at an $O(\delta_A)$ distance above the substrate, and there is a 'transition' region which matches smoothly between the adhered and outer regions and which regularises the apparent discontinuity in curvature between these regions. The membrane's height in the transition region is given by $y = O(\delta_A)$, whereas the curvature must approach the value $H = (2W_0)^{1/2}$ towards the outer region. Because the membrane has a small inclination near the substrate, we make the leading-order approximation that $H = \mathrm{d}^2h/\mathrm{d}x^2$ which implies that the horizontal lengthscale of the transition region is given by

$$\delta_X = (2W_0)^{-1/4}\delta_A^{1/2}. \tag{3}$$

Hence, regardless of the strength of the adhesive interaction, $\delta_A \ll \delta_X$ for sufficiently small δ_A, which motivates the use of lubrication theory[9] to analyse the spreading of a vesicle in the regime where $\delta_A \ll 1$.

3. Lubrication model

It is convenient from now on to use rescaled variables (denoted by tildes) to describe the motion of the underside of the vesicle, and we rescale coordinates using $x = \delta_X\widetilde{x}$ and $y = \delta_A\widetilde{y}$, pressures using $p = (2W_0/\delta_A)\widetilde{p} \equiv (\delta_A/\delta_X^4)\widetilde{p}$, horizontal velocity components using $u = (2W_0)^{5/4}\delta_A^{1/2}\widetilde{u}$ and times using $t = (2W_0)^{-3/2}\widetilde{t}$. On the substrate, we prescribe the condition that the fluid velocity is zero. On the membrane, we prescribe no slip between the membrane and the fluid. Because the membrane is locally inextensible and is assumed to have small slope, the horizontal velocity component of the membrane is approximately constant. (A rigorous but more cumbersome argument may be made by considering the tangential stress balance at the membrane[10] which demonstrates that both γ and the membrane's horizontal velocity are constant at leading order.) If we make the further assumption that the adhered part of the membrane does not move relative to the substrate, then the horizontal velocity components of both the membrane and the neighbouring fluid are zero. It can then be shown that the evolution of the membrane's height is given by

$$\frac{\partial\widetilde{h}}{\partial\widetilde{t}} = \frac{\partial}{\partial\widetilde{x}}\left[\frac{\widetilde{h}^3}{12}\frac{\partial\widetilde{p}}{\partial\widetilde{x}}\right]. \tag{4}$$

Because the aspect ratio of the thin film is small, the pressure beneath the membrane is independent of $\widetilde{y}$ at leading order, and is given by the difference between the normal viscous stress components on either side of the membrane. We use the small-slope approximations $\widetilde{H} \approx \mathrm{d}^2\widetilde{h}/\mathrm{d}\widetilde{x}^2$ and $\mathrm{d}/\mathrm{d}\widetilde{s} \approx \mathrm{d}/\mathrm{d}\widetilde{x}$, together with (2), to conclude that the (rescaled) pressure beneath the membrane is given at leading order by

$$\widetilde{p} = \frac{\partial^4\widetilde{h}}{\partial\widetilde{x}^4} - \frac{2}{\widetilde{h}^5} + \frac{2}{\widetilde{h}^3}. \tag{5}$$

3.1. Travelling-wave solutions

We seek travelling-wave solutions to (4) and (5) of the form $\widetilde{h}(\widetilde{x},\widetilde{t}) = \widetilde{h}(\widetilde{\eta})$, where $\widetilde{\eta} = \widetilde{x} - \widetilde{U}\widetilde{t}$. Such solutions satisfy the sixth-order equation

$$\left(\frac{\widetilde{h}^3}{12}\widetilde{p}'\right)' + \widetilde{U}\widetilde{h}' = 0, \quad \text{where} \quad \widetilde{p} = \widetilde{h}'''' - \frac{2}{\widetilde{h}^5} + \frac{2}{\widetilde{h}^3}, \tag{6}$$

where primes denote differentiation with respect to $\widetilde{\eta}$ and the travelling wave speed $\widetilde{U}$ is an unknown parameter. Because we have assumed that the adhesive potential is independent of the position $\widetilde{x}$ along the substrate, (6) is unchanged by translations in $\widetilde{\eta}$. Hence, only six matching conditions are needed to determine the shape of the membrane up to translations. We assume that the adhered region lies to the left of the transition region, and has constant membrane height given by $\widetilde{h}_\infty$, in which case (6) may be integrated to obtain

$$\frac{\widetilde{h}^3}{12}\widetilde{p}' + \widetilde{U}(\widetilde{h} - \widetilde{h}_\infty) = 0. \tag{7}$$

We linearise about the membrane's height in the adhered region by posing the solution $\widetilde{h} = \widetilde{h}_\infty + (\widehat{h}\mathrm{e}^{\sigma\widetilde{\eta}} + \text{c.c.})$, where $\widehat{h}$ is a small, complex-valued amplitude and where c.c. denotes the complex conjugate. Substitution of this solution into (6) implies that σ must satisfy

$$\sigma^5 + \left[\frac{10}{\widetilde{h}_\infty^6} - \frac{6}{\widetilde{h}_\infty^4}\right]\sigma + \frac{12\widetilde{U}}{\widetilde{h}_\infty^3} = 0. \tag{8}$$

Any modes which do not decay as $\widetilde{\eta} \to -\infty$ must be suppressed which, because the adhered region is assumed to lie to the left of the transition region, means that all modes for which σ has negative real part must be suppressed. In the case of an advancing wave with $\widetilde{U} > 0$, there are three roots of (8) with negative real part, and three matching conditions are thus required to suppress the corresponding modes. (In the case of a receding wave with $\widetilde{U} < 0$, there are only two roots of (8) with negative real part. Two matching conditions would be prescribed to suppress these, and a third matching condition would prescribe the value of $\widetilde{h}_\infty$ in the adhered region.) The other two roots form a conjugate pair, and a superposition of the corresponding modes may therefore be expressed in the form

$$\widetilde{h} - \widetilde{h}_\infty = \widetilde{A}\mathrm{e}^{\sigma_r\widetilde{\eta}}\cos(\sigma_i\widetilde{\eta} + \widetilde{\phi}), \tag{9}$$

where $\widetilde{A}$ is a real-valued constant which we set to a small value, σ_r and σ_i are, respectively, the real and imaginary parts of σ, and $\widetilde{\phi}$ is a phase shift which represents the relative contribution of the conjugate mode. We use (9) to prescribe the values of $\widetilde{h}$ and its first four derivatives at $\widetilde{\eta} = 0$, and then adjust the values of $\widetilde{h}_\infty$, $\widetilde{\phi}$ and $\widetilde{U}$ in order to satisfy matching conditions towards the outer region which we now describe. We treat the outer region as quasi-static, with a prescribed membrane curvature $\widetilde{H}_c$, which requires $\widetilde{h}''' = O(\delta_X)$ and $\widetilde{h}'''' = O(\delta_X^2)$ as $\widetilde{\eta} \to \infty$. In our numerical solution, we approximate these matching conditions by enforcing the conditions

$$\widetilde{h}'' = \widetilde{H}_c, \quad \widetilde{h}''' = 0 \quad \text{and} \quad \widetilde{h}'''' = 0 \quad \text{at} \quad \widetilde{h} = \widetilde{h}_{\text{out}} \gg 1, \tag{10}$$

and we use the values $\widetilde{A} = 10^{-7}$ and $\widetilde{h}_{\text{out}} = 2 \times 10^3$. The results are insensitive to the precise value of $\widetilde{A}$. Although we are matching towards a height profile of the form $\widetilde{h} \sim \frac{1}{2}\widetilde{H}_c\widetilde{\eta}^2 + B\widetilde{\eta} + C$, if $\widetilde{H}_c$ is small then the quadratic nature of this profile is only apparent for large values of $\widetilde{\eta}$, and so large values of $\widetilde{h}_{\text{out}}$ are needed to fully resolve $\widetilde{U}$. We find that for $\widetilde{h}_{\text{out}} = 5 \times 10^3$, the dependence of $\widetilde{U}$ on $\widetilde{H}_c$ has converged (to within the width of the line) for values of $\widetilde{H}_c$ greater than around 5×10^{-2}.

3.2. Estimation of spreading

Fig. 2(a) shows the dependence of the travelling wave speed $\widetilde{U}$ on the rescaled curvature $\widetilde{H}_c$. We note that the case where $\widetilde{H}_c = 1$ and $\widetilde{U} = 0$ corresponds to $H_c = (2W_0)^{1/2}$ in the unscaled variables, which is the equilibrium curvature[4] that the membrane in the outer region would have as it approaches the substrate in the limiting case that

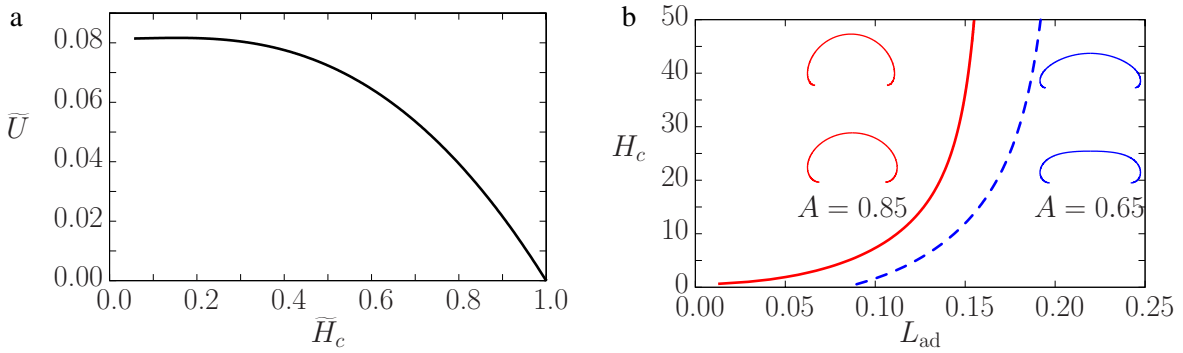

Fig. 2. (a) The dependence of the travelling wave speed $\widetilde{U}$ of the transition region on the curvature $\widetilde{H}_c$ of the membrane far from the substrate. The values of $\widetilde{U}$ for $\widetilde{H}_c \lesssim 5 \times 10^{-2}$ have not fully converged for the computational domain used to solve (7). (b) The dependence of the (unscaled) curvature H_c of the membrane on the adhered length $L_{\rm ad}$ of the membrane, for specific areas $A = 0.85$ (solid) and 0.65 (dashed).

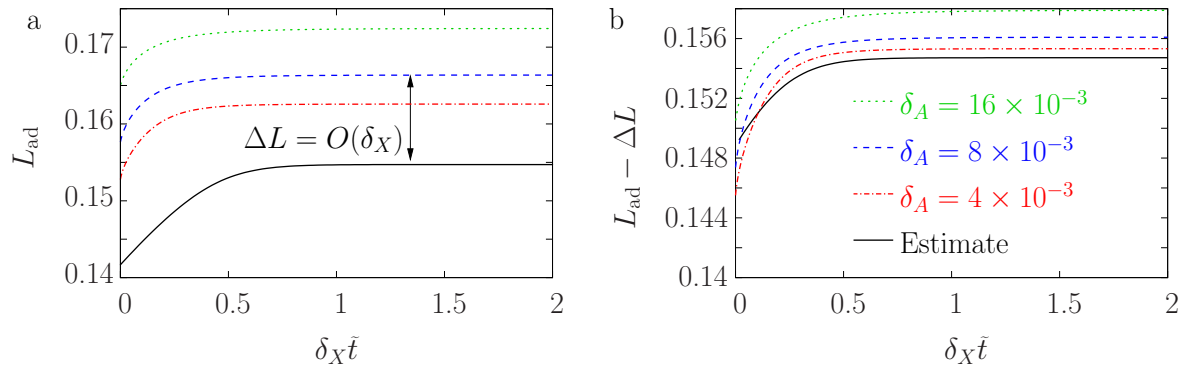

Fig. 3. Comparison of the lubrication model with boundary-integral simulations during the spreading phase. Parameter values used are $W_0 = 1200$ and $A = 0.85$. (a) The adhered half-length $L_{\rm ad}$ estimated using (12) (solid), and obtained directly from the boundary-integral simulations for various values of δ_A (Dotted: 16×10^{-3}. Dashed: 8×10^{-3}, Chain-dashed: 4×10^{-3}). (b) The same plot as (a), except that the estimate from (12) are offset in time by an amount that is determined by a visual fit, and the estimates from the boundary-integral simulations are offset by the $O(\delta_X)$ contribution to $L_{\rm ad}$ of the transition region in equilibrium.

$\delta_A = 0$. Fig. 2(b) shows the dependence of H_c on the adhered half-length $L_{\rm ad}$ (measured from the centre of the adhered region to the contact point) of the membrane in contact with the substrate, computed using a contact-potential model[4]. Two different values of the specific area A are used, where A is defined to be $4\pi A^*/P^{*2}$ and represents the area of the vesicle, scaled by the area the vesicle would have if it were circular and had the same perimeter.

The spreading behaviour of the vesicle may be estimated by assuming that the outer region evolves quasi-statically. If H_c differs from the equilibrium value $(2W_0)^{1/2}$ then the vesicle will either spread out, which would increase H_c, or retract, which would decrease H_c. The spreading rate is given in scaled variables by $\widetilde{U}[\widetilde{H}_c]$. As the vesicle spreads, its adhered half-length $L_{\rm ad}$ increases, thereby increasing H_c and, in turn, decreasing the travelling wave speed U until it reaches zero and the contact curvature attains its equilibrium value of $(2W_0)^{1/2}$. The rate of change of $L_{\rm ad}$ may therefore be estimated by solving the implicit equation

$$\frac{{\rm d}L_{\rm ad}}{{\rm d}t} = W_0^{5/4}\delta_A^{1/2}\widetilde{U}[\widetilde{H}_c(L_{\rm ad})], \quad \text{where} \quad \widetilde{H}_c = \frac{H_c(L_{\rm ad})}{(2W_0)^{1/2}}, \tag{11}$$

where $\widetilde{U}[\widetilde{H}_c]$ and $H_c(L_{\rm ad})$ are plotted in Fig. 2 and must be computed numerically.

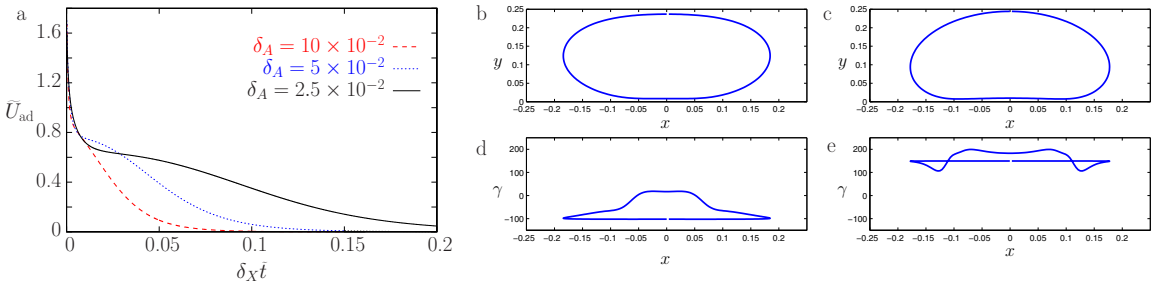

Fig. 4. (a) Estimate of the contact-line speed during the attachment phase, obtained using boundary-integral simulations. Parameter values used are $W_0 = 10$, $A = 0.85$, and $\delta_A = 2.5 \times 10^{-2}$ (solid), 5×10^{-2} (dotted) and 10×10^{-2} (dashed). (b–e) The vesicle's shape (b,c) and tension distribution (d,e) at two times during the attachment of a vesicle to a substrate.

3.3. Comparison with boundary-integral simulations

Integration of (11) yields

$$L_{\rm ad} = \int W_0^{5/4} \delta_A^{1/2} \widetilde{U}[\widetilde{H}_c(L_{\rm ad})]\, {\rm d}t \equiv \int \widetilde{U}[\widetilde{H}_c(L_{\rm ad})]\, {\rm d}(\delta_X \widetilde{t}), \tag{12}$$

which gives an implicit equation for $L_{\rm ad}$ in terms of $\delta_X \widetilde{t}$. Fig. 3(a) shows the solution of this equation for a vesicle with specific area given by $A = 0.85$, and with the amplitude of the adhesive potential given by $W_0 = 1200$. The initial value of $L_{\rm ad}$ is 0.142, which corresponds to the equilibrium adhered length the vesicle would have in the case that $W_0 = 300$ and in the limiting case of a contact potential with $\delta_A = 0$.

To verify the accuracy of our estimate, we also computed the evolution of the membrane's shape $\boldsymbol{x}(s,t)$ by solving the boundary-integral equation

$$\frac{{\rm d}\boldsymbol{x}}{{\rm d}t} = \int \boldsymbol{G}(\boldsymbol{x}-\boldsymbol{y}) \cdot \{\boldsymbol{\sigma}\cdot\boldsymbol{n}|_{\rm out} - \boldsymbol{\sigma}\cdot\boldsymbol{n}|_{\rm in}\}(\boldsymbol{y})\, {\rm d}s_{\boldsymbol{y}}. \tag{13}$$

In (13), the integral kernel $\boldsymbol{G}$ is the Blake–Oseen tensor[11], which includes 'image' singularities to represent the presence of the rigid substrate in the present problem, and the stress discontinuity across the membrane is given explicitly by (2). For simplicity, we have assumed that the fluid viscosities are equal inside and outside the vesicle, thereby omitting the double-layer term that would otherwise be present. (The viscosity of fluid inside the vesicle is unlikely to play a significant role because the dynamics are dominated by the thin-film flow beneath the vesicle.) The computational solution of (13) uses a similar implementation to that used recently to compute the behaviour of a two-dimensional suspension of vesicles[12]. The procedure involves discretising the membrane using equally spaced points along its arclength, and evaluating the nearly singular integrals that arise using a hybrid Gauss-trapezoidal quadrature rule[13].

The adhered length is estimated from the boundary-integral calculations using $L_{\rm ad} = (2W_0)^{-1} \int W\, {\rm d}s$, and is shown in Fig. 3(a). The simulations are performed using $\delta_A = 4 \times 10^{-3}$, 8×10^{-3} and 16×10^{-3}. In each case, the specific area and adhesive energy used are $A = 0.85$ and $W_0 = 1200$, respectively, and each simulation is initialised with the equilibrium shape that the vesicle would have if $W = 300$. As described in Sec. 2.1, these equilibrium solutions include transition regions, which at leading order[6] give a contribution to $L_{\rm ad}$ of $\Delta L = 1.745\delta_X$. This correction should be added to the estimate (12) to allow a direct comparison between each boundary-integral simulation and the corresponding estimate using (12). However, for ease of presentation, Fig. 3(b) instead shows plots where ΔL has been subtracted from the computed values of $L_{\rm ad}$. Fig. 3(a) shows that there is also a discrepancy between the dependence of the adhered length on time. This may be attributed to a transient motion during which the travelling-wave behaviour (assumed by the estimate 12) has not been attained. In Fig. 3(b) this estimate has, therefore, been translated in time by an amount that is obtained using a visual fit. There is a good collapse of the data towards this estimate, which indicates that (12) does indeed give a good description of the spreading of the vesicle along the substrate.

In general, the process by which a vesicle adheres to a substrate is analogous to that of a viscous droplet[7], and begins with a transient behaviour where the vesicle first drifts towards the substrate owing to the long-range attraction

of the adhesive interaction, before being strongly deformed by gradients in the adhesive potential as it approaches the substrate. To assess the applicability of the lubrication model to this part of the motion, boundary-integral simulations were initialised with a vesicle whose shape was that of an isolated vesicle in equilibrium, located so that its minimum distance from the substrate was at $y = \delta_A$. Fig. 4(a) shows the variation of the contact-line speed, estimated using $U_{\mathrm{ad}} = \mathrm{d}L_{\mathrm{a}}/\mathrm{d}t$, with rescaled time $\delta_X \widetilde{t}$. Although there seems to be a collapse for very short times, it is clear that a lubrication model does not adequately describe the evolution of the membrane throughout the motion.

4. Discussion

A lubrication approximation has been used to model the motion of a vesicle as it attaches to a horizontal substrate, and travelling-wave solutions have been found. A comparison with boundary-integral simulations suggests that these solutions may only be applied to situations where the vesicle is near equilibrium. We therefore expect that the results obtained here may be used to estimate the spreading of a vesicle at late stages in the adhesion process. A simple extension to our work lies in computing receding travelling-wave solutions in addition to advancing ones. We anticipate that such solutions represent the retraction of the vesicle's contact area during detachment processes. The detachment of a vesicle from a substrate has been studied experimentally[2], and it was found that for deflated vesicles, the thickness of the film beneath the vesicle remains constant as the contact radius decreases. This reported behaviour supports our modelling of the adhesive process as being dominated by the edges of the contact region. It should be noted that these observations relate only to 'deflated' vesicles, for which the membrane's bending stiffness plays a significant role. In regimes where the vesicle is 'tensed', such as when the adhesive interaction is very strong[3], the membrane's bending stiffness is unimportant and the dynamics are governed instead by the membrane's tension. In this regime, the thickness of the entire film increases at approximately the same rate whereas the contact radius remains constant. One other application of our results lies in the forced translation of a vesicle along a substrate by a shear flow, or by a gradient in the adhesive strength[8]. If the film thickness beneath the vesicle is small, then we anticipate that the vesicle will undergo a rolling motion in which the membrane on the underside remains at rest with the dynamics dominated by an advancing contact region at the front of the vesicle and a receding contact region at the rear. An understanding both of vesicle detachment and of vesicle translation would require an analysis of receding travelling-wave solutions and of the effects of an external flow, both of which represent extensions to the results presented here.

The estimates we have obtained using travelling-wave solutions work well in cases where the vesicle's shape is already close to its equilibrium shape, but in general the flow beneath the vesicle is not well described by lubrication theory. We attribute this to the assumptions made in Sec. 3.1 that the adhered region is at rest and that the membrane there is horizontal. In general, this is not the case, because the lubrication pressure that drives fluid out from beneath the vesicle also has the effect of deforming the underside of the vesicle. This causes a dimple of fluid to be trapped, in an analogous way to the observed behaviour of viscous droplets[14,15], which precludes the formation of an adhered region. Dimple formation in the context of the adhesion of vesicles has been observed experimentally[16].

Fig. 4(b–e) shows the membrane shape and tension at early and late times during a boundary-integral simulation of vesicle adhesion, and shows that there is significant variation in the tension along the underside of the vesicle. The role of the membrane's tension is to enforce local inextensibility and, because a small-slope approximation automatically implies length conservation at leading order, we conclude that significant gradients in the membrane tension would imply that the small-slope approximation used in Sec. 3.1 is not valid. However, the simulations also demonstrate that the tension in the outer region is constant, which supports our use of a quasi-static approximation to describe this region.

The flow beneath a viscous droplet that sediments under gravity towards a rigid substrate has been analysed using a modified lubrication theory[15]. In that problem, fluid is trapped beneath the droplet to form finite-amplitude 'dimples', and a model was developed that incorporates finite-amplitude expressions for the curvature of the interface. This model was justified by the dynamics being controlled by thin 'neck' regions where the slope is small, and by the dimples, where the slope is significant, behaving quasi-statically. It is feasible that a similar approach could be used to describe to the flow beneath adhering vesicles, though the implementation would be complicated by the membrane tension not being known in advance. The development of a modified lubrication model theory to describe the fluid flow underneath a vesicle is ongoing.

One important aspect that has not been considered here is the influence of thermal fluctuations. In contrast to the strongly-adhered regime considered recently by other workers[3], the adhesive interactions analysed here are not sufficiently large to place the vesicle in a 'tensed' regime in which thermal fluctuations are suppressed. A topic for future investigation is the extent to which fluctuations of the membrane might affect the process by which a vesicle adheres to a substrate, and how these fluctuations might be described using a mean-field theory.

The analysis performed here has been applied to the relatively simple process of an isolated vesicle adhering to a stationary substrate. A lubrication model has been used to analyse the motion of a fluid droplet near a rigid wall in a variety of situations including the rolling of a droplet down a slope[17] and the motion of a droplet through a tube[18], and an interesting extension of these works would be to adapt them to describe vesicles or capsules. In either case, the development of the model is complicated by the coupling between the viscous traction exerted on the interface and its stretching or contraction.

Acknowledgements

This work was supported by the National Institutes for Health through grant number 5R01GM086886.

References

1. Frostad, J.M., Colins, M.C., Leal, L.G.. Cantilevered-capillary force apparatus for measuring multiphase fluid interactions. *Langmuir* 2013;**29**:4715–4725.
2. Chatkaew, S., Georgelin, M., Jaeger, M., Leonetti, M.. Dynamics of vesicle unbinding under axisymmetric flow. *Phys Rev Lett* 2009; **103**:248103.
3. Ramachandran, A., Anderson, T.H., Leal, L.G., Israelachvili, J.N.. Adhesive interactions between vesicles in the strong adhesion limit. *Langmuir* 2011;**27**:59–73.
4. Seifert, U.. Adhesion of vesicles in two dimensions. *Phys Rev A* 1991;**43**:6803–6814.
5. Dussan V., E.B., Davis, S.H.. The motion of a fluid-fluid interface along a solid surface. *J Fluid Mech* 1974;**65**:71–95.
6. Blount, M.J., Miksis, M.J., Davis, S.H.. The equilibria of vesicles adhered to substrates by short-ranged potentials. *Proc Roy Soc A* 2013; **469**:20120729.
7. Hodges, S.R., Jensen, O.E.. Spreading and peeling dynamics in a model of cell adhesion. *J Fluid Mech* 2002;**460**:381–409.
8. Cantat, I., Kassner, K., Misbah, C.. Vesicles in haptotaxis with hydrodynamical dissipation. *Eur Phys J E* 2003;**10**:175–189.
9. Oron, A., Davis, S.H., Bankoff, S.G.. Long-scale evolution of thin liquid films. *Rev Mod Phys* 1997;**69**:931–980.
10. Blount, M.J., Miksis, M.J., Davis, S.H.. Fluid flow beneath a semipermeable membrane during drying processes. *Phys Rev E* 2012; **85**:016330.
11. Blake, J.R.. A note on the image system for a stokeslet in a no slip boundary. *Proc Camb Phil Soc* 1971;**70**:303–310.
12. Veerapaneni, S.K., Gueyffier, D., Zorin, D., Biros, G.. A boundary integral method for simulating the dynamics of inextensible vesicles suspended in a viscous fluid in 2D. *J Comp Phys* 2009;**228**(7):2334–2353.
13. Alpert, B.K.. Hybrid gauss-trapezoidal quadrature rules. *SIAM Journal on Scientific Computing* 1999;**20**:1551–1584.
14. Ascoli, E.P., Dandy, D.S., Leal, L.G.. Buoyancy-driven motion of a deformable drop toward a planar wall at low reynolds number. *J Fluid Mech* 1990;**213**:287–311.
15. Lister, J.R., Morrison, N.F., Rallison, J.M.. Sedimentation of a two-dimensional drop towards a rigid horizontal plane. *J Fluid Mech* 2006; **552**:345–351.
16. Streicher, P., Nassoy, P., Bärmann, M., Dif, A., Marchi-Artzner, V., Brochard-Wyart, F., et al. Integrin reconstituted in GUVs: A biomimetic system to study initial steps of cell spreading. *BBA-Biomembranes* 2009;**1788**:2291–2300.
17. Hodges, S.R., Jensen, O.E., Rallison, J.M.. Sliding, slipping and rolling: the sedimentation of a viscous drop down a gently inclined plane. *J Fluid Mech* 2004;**512**:95–131.
18. Hodges, S.R., Jensen, O.E., Rallison, J.M.. The motion of a viscous drop through a cylindrical tube. *J Fluid Mech* 2004;**501**:279–301.